



Available online at www.sciencedirect.com

ScienceDirect

**NUCLEAR
PHYSICS**

A

ELSEVIER

Nuclear Physics A 971 (2018) 1–20

www.elsevier.com/locate/nuclphysa

Production of ^4He and $^4\overline{\text{He}}$ in Pb–Pb collisions at $\sqrt{s_{\text{NN}}} = 2.76 \text{ TeV}$ at the LHC

ALICE Collaboration*

Received 26 October 2017; received in revised form 20 December 2017; accepted 21 December 2017

Available online 27 December 2017

Abstract

Results on the production of ^4He and $^4\overline{\text{He}}$ nuclei in Pb–Pb collisions at $\sqrt{s_{\text{NN}}} = 2.76 \text{ TeV}$ in the rapidity range $|y| < 1$, using the ALICE detector, are presented in this paper. The rapidity densities corresponding to 0–10% central events are found to be $dN/dy_{^4\text{He}} = (0.8 \pm 0.4 \text{ (stat)} \pm 0.3 \text{ (syst)}) \times 10^{-6}$ and $dN/dy_{^4\overline{\text{He}}} = (1.1 \pm 0.4 \text{ (stat)} \pm 0.2 \text{ (syst)}) \times 10^{-6}$, respectively. This is in agreement with the statistical thermal model expectation assuming the same chemical freeze-out temperature ($T_{\text{chem}} = 156 \text{ MeV}$) as for light hadrons. The measured ratio of $^4\overline{\text{He}}/{}^4\text{He}$ is $1.4 \pm 0.8 \text{ (stat)} \pm 0.5 \text{ (syst)}$.

© 2018 Elsevier B.V. This is an open access article under the CC BY license (<http://creativecommons.org/licenses/by/4.0/>).

Keywords: Pb–Pb collisions; ALICE detector; LHC; Anti-nuclei

1. Introduction

The production of light (hyper-)nuclei, up to a mass number $A = 3$, has been reported already in Pb–Pb collisions at $\sqrt{s_{\text{NN}}} = 2.76 \text{ TeV}$ at the Large Hadron Collider (LHC). This includes deuterons, ${}^3\text{He}$ and the hypertriton as well as their corresponding anti-particles [1,2]. The observed total yields can be described well by equilibrium thermal models [3–9], with only three free parameters: the chemical freeze-out temperature T_{chem} , the volume V and the baryo-chemical potential μ_B . The current best fit to the measured yields at the LHC, including results ranging in mass from pions up to ${}^3\text{He}$, results in a $T_{\text{chem}} = 156 \text{ MeV}$ [10]. The measurement of the production yields of ${}^4\text{He}$ and ${}^4\overline{\text{He}}$ ($A = 4$) will put additional constraints on T_{chem} . Since the baryo-chemical potential is consistent with zero ($\mu_B = 0.7 \pm 3.8 \text{ MeV}$ [11]) at LHC energies,

* E-mail address: alice-publications@cern.ch.

the expected anti-baryon to baryon ratio is unity. Therefore, also the ratio is expected to be close to unity for particles composed of (anti-)baryons, namely the anti-nuclei and nuclei [6].

Furthermore, ${}^4\overline{\text{He}}$ is the heaviest anti-nucleus ever observed. It was discovered in Au–Au collisions at RHIC by the STAR Collaboration [12]. Out of 10^9 Au–Au collisions at centre-of-mass energies per nucleon pair ($\sqrt{s_{\text{NN}}}$) of 200 GeV and 62.4 GeV, 18 ${}^4\overline{\text{He}}$ have been detected. The corresponding yield at a given transverse momentum p_T is compared to the prediction of the thermal model [13] and the coalescence nucleosynthesis model [14] and found to be consistent with both. A confirmation of this observation is still pending as no other experiment has been able to detect the ${}^4\overline{\text{He}}$ particle since then.

Coalescence models have been successfully used to describe the general trends of deuteron production [15–25] in relativistic nuclear collisions, albeit with a number of external parameters. These models are clearly challenged with the regular pattern observed in the production probability for light nuclei measured by the STAR [12] and ALICE [1] Collaborations. To extend the studies to $A = 4$ the measurement at LHC energies is obviously of great interest.

In this paper, the measurement of the production yield of the ${}^4\text{He}$ and ${}^4\overline{\text{He}}$ nuclei with the ALICE apparatus is presented. Besides the increase in collision energy, the main difference with respect to the measurement by the STAR Collaboration is the usage of a six layer silicon vertex detector in ALICE. Together with the other barrel detectors this provides precision information on vertex position, particle identification and momentum. The determined yields are compared to thermal model expectations.

2. Detector setup and data sample

The two main detectors involved in the identification of the ${}^4\text{He}$ and ${}^4\overline{\text{He}}$ particles are the Time Projection Chamber (TPC) [26] and the Time of Flight (TOF) detector [27], combined with the start time detector T0. In addition, V0 detectors ([28,29]) are used for centrality determination and the Inner Tracking System (ITS) [30] is employed for tracking and the discrimination between primary and secondary particles [1,31]. A full description of the ALICE detector can be found in [32], whereas the performance of the ALICE sub-detectors is reported in [33].

The measurement of the ${}^4\text{He}$ and ${}^4\overline{\text{He}}$ particles is performed on the 2011 data set of Pb–Pb collisions at $\sqrt{s_{\text{NN}}} = 2.76$ TeV. From this campaign, 38.7×10^6 events in a trigger mix of central, semi-central and minimum-bias events are used in this analysis. This leads to 20.7×10^6 events in the 0–10% centrality interval, 17.4×10^6 events in the 10–50% centrality interval and 0.6×10^6 events in the 50–80% centrality interval. The combined yields are extrapolated to the 0–10% centrality class with the procedure discussed in section 4.

3. Analysis

To ensure high tracking efficiency, high energy-deposit (dE/dx) resolution in the TPC and a good track matching between the TPC and TOF detectors, a set of selection criteria is applied. In order to select primary particles, the corresponding tracks have to originate from the primary vertex. The primary vertex position is estimated using the ITS and the TPC detectors. The resolution of the vertex determination is better than $50 \mu\text{m}$ in the xy-plane and $150 \mu\text{m}$ in the z-direction for charged particles with momenta above $1 \text{ GeV}/c$. To select primary tracks, the minimum distance from the vertex, called Distance-of-Closest-Approach (DCA), is required to be smaller than 1 cm along the z-axis, whereas the DCA in the xy-plane must not be greater than 0.1 cm. In addition, a hit in the TOF detector is required for a precise time measurement and only those tracks are used for the track reconstruction. The selection criteria are summarised in Table 1.

Table 1
Selection criteria applied for the ${}^4\text{He}$ and ${}^4\overline{\text{He}}$ analyses.

Track selection criteria	value
Number of clusters in TPC	$n_{\text{cl}} > 80$
Number of hits in ITS	$n_{\text{hits}} > 2$
TPC track quality	$\chi^2/\text{cluster} < 4$
Acceptance in pseudo-rapidity	$ \eta < 0.8$
Acceptance in rapidity	$ y < 1$
DCA _z	$\text{DCA}_z < 1\text{ cm}$
DCA _{xy}	$\text{DCA}_{xy} < 0.1 \text{ cm}$
PID selection	value
TPC PID cut	$\pm 3\sigma$
TOF mass window	$\pm 3\sigma$

The dE/dx is measured in the TPC as a function of the rigidity p/z , where p is the momentum and z is the electric charge in units of the elementary charge e . This distribution of reconstructed charged particles is well described by the Bethe–Bloch formula [34,35] and is unique for each particle species.

Primarily, all events with at least one particle with a dE/dx corresponding to a ${}^3\text{He}$ and ${}^3\overline{\text{He}}$ or a higher mass are selected. To ensure a good track matching between the TPC and the TOF detectors, only candidates within 3 standard deviations (σ) around the mean in the dE/dx (TPC) vs. $\beta\gamma$ (TOF) plane are accepted. Here, β denotes the relativistic velocity $\beta = v/c$ and γ is the Lorentz factor. In order to select ${}^4\text{He}$ or ${}^4\overline{\text{He}}$ particles, candidates within a 3σ band of the Bethe–Bloch parametrisation in the dE/dx versus p/z distribution are taken into account. At higher momenta, the two Bethe–Bloch curves of ${}^4\text{He}$ or ${}^4\overline{\text{He}}$ and of ${}^3\text{He}$ or ${}^3\overline{\text{He}}$ approach each other. To study a possible contamination from ${}^3\text{He}$ and ${}^3\overline{\text{He}}$ particles, different narrower cuts for the TPC dE/dx selection band are investigated: while the upper cut of the band (3σ) is fixed, the lower cut is restricted progressively going in steps of 0.5 units from -3σ up to 0σ . For all these seven cuts the procedure described in the following is carried out and a yield dN/dy is determined.

In Fig. 1, the velocity (β) distributions of He candidates are plotted versus rigidity. One can clearly see the separation of ${}^3\text{He}$ and ${}^4\text{He}$. From these data, the m^2/z^2 (m = mass of the particle) distributions are calculated and displayed in the insert of this figure. From the insert, the separation of ${}^3\text{He}$ and ${}^4\text{He}$ can be quantitatively asserted. The m^2/z^2 is different for ${}^3\text{He}$ ($2.00 \text{ GeV}^2/c^4$) and ${}^4\text{He}$ ($3.48 \text{ GeV}^2/c^4$). Candidates lying within a window of $2.86 \text{ GeV}^2/c^4 < m^2/z^2 < 4.87 \text{ GeV}^2/c^4$ are identified as ${}^4\text{He}$ or ${}^4\overline{\text{He}}$ particles. This window is determined by a fit to the peak in the m^2/z^2 distribution of the selected tracks. Because of the low statistics, the fitting is done simultaneously both for particles and for anti-particles, including secondary ${}^4\text{He}$ knocked out from the material. A Gaussian with an exponential tail on the right side is used as the fit function. For the background, the sum of a first-order polynomial and an exponential shape is assumed. This is necessary to describe the time-signal shape of the TOF detector [27]. The polynomial shape is needed to cope with mismatched candidate tracks in the signal region. A similar procedure is used in [1].

For the analysis of positively charged ${}^4\text{He}$, contamination from ${}^4\text{He}$ nuclei which do not originate from the primary vertex, but stem from the detector material due to knockout processes, are taken into account. Monte Carlo studies suggest a cut on $p/z > 2 \text{ GeV}/c$ to eliminate such

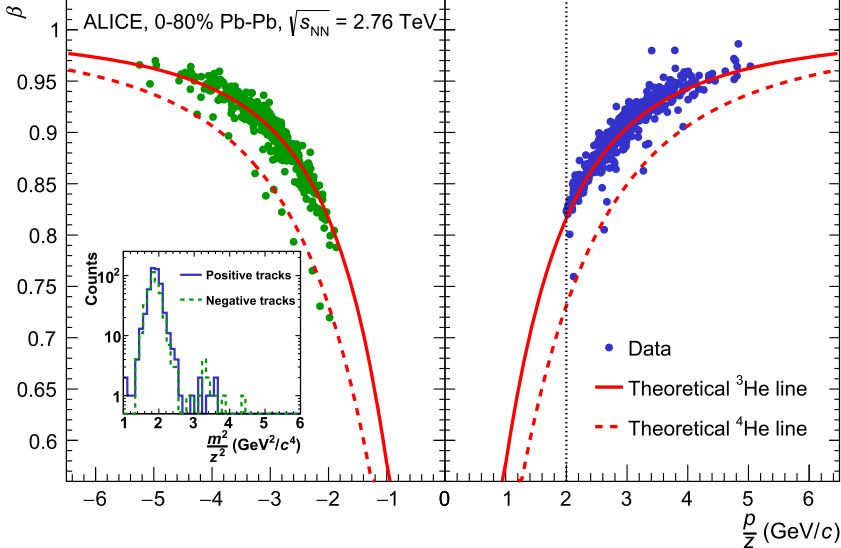


Fig. 1. Velocity β measured with the TOF detector as a function of the rigidity p/z . For this figure a selection band of -1.5 to 3σ around the mean of the TPC specific energy-loss distribution is required. Negatively (positively) charged particles are shown on the left (right) side, with positive tracks in blue and negative tracks in green. The dashed vertical line represents the cut on the rigidity $p/z = 2 \text{ GeV}/c$ (applied only for positively charged particles). The insert shows the m^2/z^2 distributions obtained from the data points shown in the main figure. (For interpretation of the references to colour in this figure legend, the reader is referred to the web version of this article.)

a background. Note that the background due to knockout processes is steeply falling with momentum and the signal is rising in this momentum range. Therefore, only ${}^4\text{He}$ candidates with a p/z greater than $2 \text{ GeV}/c$ are accepted. The contamination at higher momenta is estimated to be a maximum of 0.13 counts out of a total count of the order of 10, which is added as a systematic uncertainty.

The small number of clear signal counts observed by combining the TPC and TOF information does not give any indication of background. In order to estimate an upper limit on the background counts from mismatched tracks in the TOF detector underneath the ${}^4\text{He}$ or ${}^{4\bar{\text{He}}}$ peak in the TOF mass window, a likelihood fit under the assumption of a flat background is performed in the dE/dx versus $\beta\gamma$ plane outside the $\pm 3\sigma$ matching band. In this way, background candidates are identified as mismatched particles. (These are usually rejected and only used for this purpose.) Due to limited statistics, this procedure cannot be used if a stronger selection criterion is applied for the TPC dE/dx selection, since no ${}^4\text{He}$ or ${}^{4\bar{\text{He}}}$ candidates are left to apply this technique. For these particular cases, we assume a constant ratio of ${}^3\text{He}$ to background counts and use this to estimate the number of ${}^4\text{He}$ background.

The background stemming from misidentification of (anti-) ${}^3\text{He}$ as (anti-) ${}^4\text{He}$ is estimated to be more than one order of magnitude smaller than the one from the mismatch of TPC tracks when extrapolated to the TOF detector and is therefore considered to be negligible. The estimated background decreases with more stringent TPC dE/dx cuts. The signal-to-background ratio improves depending on the tightness of the dE/dx cut from 1.7 to 8.4 for ${}^4\text{He}$ and from 1.7 to 17.6 for ${}^{4\bar{\text{He}}}$.

To estimate the efficiency for the detection of ${}^4\text{He}$ and ${}^{4\bar{\text{He}}}$, a Monte Carlo simulation is generated in which the kinematical distributions of the particles are generated flat both in rapidity

y and in transverse momentum p_T . The shape of p_T spectra in heavy-ion collisions is typically described by a blast-wave model [36]. This model assumes an average radial-flow velocity $\langle \beta \rangle$ and a kinetic freeze-out temperature T_{kin} as described in [37]. Generally, most hadron p_T spectra measured in heavy-ion collisions can be described well by one common set of parameters [38]. Surprisingly, this also works well for the description of deuteron and ^3He p_T spectra [1]. Hence the same prescription is used here for the p_T shape of ^4He and $^4\overline{\text{He}}$ particles, namely the same set of parameters is used, only the mass is changed to the ^4He mass.

Since only a small number of ^4He and $^4\overline{\text{He}}$ particles (14 $^4\overline{\text{He}}$ and 9 ^4He for the widest TPC dE/dx cut) are observed, a p_T spectrum can not be measured. It is estimated using the blast-wave parameters of deuterons and ^3He spectra [1]. The final acceptance \times efficiencies are obtained as described in [39] and are of the order of 15% for ^4He and 20% for $^4\overline{\text{He}}$. The difference originates from the 2 GeV/c rigidity cut applied to ^4He candidates.

For the $^4\overline{\text{He}}$ analysis, the absorption in the detector material is taken into account using two different transport codes, namely GEANT3 [40] and GEANT4 [41]. These two codes use different models for the estimation of the absorption cross section. In GEANT4, a Glauber model based on the well known hadronic interaction cross sections for (anti-)protons is implemented [42]. The version of GEANT3 used in this analysis is modified [1] such that it calculates the absorption based on an empirical parameterisation [43], based on the measurements of anti-deuterons carried out at Serpukhov [44]. The baseline is given by the absorption calculated with GEANT4, while the GEANT3 based correction is used in the systematic uncertainty evaluation. The maximum absorption probability towards low p/z is about 20%. In contrast to GEANT4, which still shows an absorption of about 5% at $p_T = 10$ GeV/c, GEANT3 exhibits basically no absorption above 3.5 GeV/c.

The main contributions to the systematic uncertainty on the determined production yields are:

- The uncertainty due to the unknown shape of the p_T distributions, which is determined by using the blast-wave model based on the measured deuteron and ^3He spectra [1]. This leads to a systematic uncertainty contribution of around 13%.
- Only for ^4He : The rigidity cut on p/z greater than 2 GeV/c itself has a systematic uncertainty of 4 to 13% depending on the TPC PID cut. As mentioned before, the secondary contamination above this cut is estimated to be a maximum of 0.13 counts. This leads to a systematic uncertainty of at minimum 20% and at maximum 49% growing with stricter TPC PID cut. As the number of observed candidates shrinks with stricter TPC dE/dx selection, the systematic uncertainty on the secondary contamination grows.
- Only for $^4\overline{\text{He}}$: The absorption correction has an uncertainty of 7%, estimated from the difference of the two GEANT implementations.

Other systematic uncertainties are estimated by varying the cuts in the limits consistent with the detector resolution. The contributions of these systematic uncertainties are typically found to be below the percent range. The systematic uncertainty on the chosen TPC PID cut varies between 1% for the most loose cuts and 19% for stricter cuts. This is caused by the stronger sensitivity of the stricter cuts, namely the even further reduced low number of candidates, which is not reflected in the Monte Carlo simulation.

The final values and the corresponding uncertainties are calculated as a mean from the previously discussed variations of the selection criteria. The resulting systematic uncertainty on the final yield is 35% for ^4He and 20% for $^4\overline{\text{He}}$.

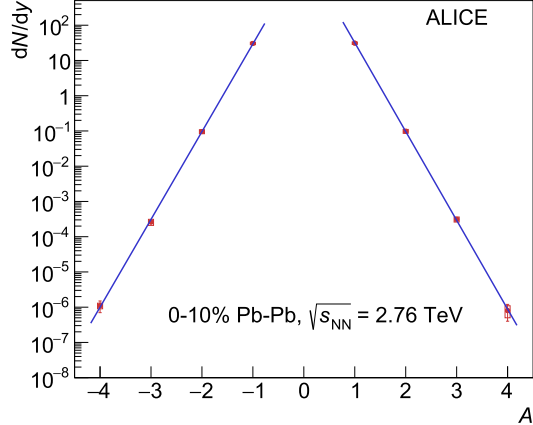


Fig. 2. dN/dy for protons ($A = 1$) up to ${}^4\text{He}$ ($A = 4$) and the corresponding anti-particles in central (0–10%) Pb–Pb collisions at $\sqrt{s_{\text{NN}}} = 2.76$ TeV. The blue lines are fits with an exponential function. Statistical uncertainties are shown as lines, whereas the systematic uncertainties are represented by boxes.

4. Results

The measurement is performed on a data set including central, semi-central and minimum-bias triggered events. To make use of all the data analysed, the semi-central and minimum-bias events have been extrapolated to 0–10% centrality interval assuming that the particle and anti-particle yields scale linearly with the charged-particle multiplicity $dN_{\text{ch}}/d\eta$. This procedure has already been tested to work well for the (anti-)hypertriton production [2]. In addition, d/p and ${}^3\text{He}/p$ ratios are measured to be approximately flat versus multiplicity within uncertainties [1]. Thus, for each centrality class, the number of analysed events is multiplied by the corresponding measured charged-particle density $dN_{\text{ch}}/d\eta$ [28]. If this is added up and divided by the total number of measured events it leads to a weighting factor of 1034. To get the final yield in the 0–10% centrality class the measured yield is multiplied with the $dN_{\text{ch}}/d\eta$ for 0–10% centrality (1447.5) and divided by the weighting factor, as $dN/dy_{0-10\%} = dN/dy_{\text{measured}} \times 1447.5/1034$.

This leads to final values of $dN/dy_{{}^4\text{He}} = (0.8 \pm 0.4 \text{ (stat)} \pm 0.3 \text{ (syst)}) \times 10^{-6}$ for ${}^4\text{He}$ and $dN/dy_{{}^4\overline{\text{He}}} = (1.1 \pm 0.4 \text{ (stat)} \pm 0.2 \text{ (syst)}) \times 10^{-6}$ for ${}^4\overline{\text{He}}$. For the ratio ${}^4\overline{\text{He}}/{}^4\text{He}$ we obtain $1.4 \pm 0.8 \text{ (stat)} \pm 0.5 \text{ (syst)}$ (“stat” and “syst” indicate the statistical and the systematic uncertainty).

The measured yields in the 0–10% centrality interval are shown in Fig. 2 together with those of (anti-)protons, (anti-)deuterons and (anti-) ${}^3\text{He}$ [1,38] (details on the extrapolation to 0–10% centrality can be found in [10]). The blue lines are exponential fits with the fit function Ke^{BA} resulting in $B = -5.8 \pm 0.2$, which corresponds to a penalty factor (suppression factor of production yield for nuclei with one additional baryon) of around 300. The same penalty factor is also obtained if the fit is done up to ${}^3\text{He}$ only [1].

The obtained penalty factor of around 300 for each additional nucleon is consistent with $T_{\text{chem}} \approx 160$ MeV in the equilibrium thermal models. The measured yields for ${}^4\text{He}$ and ${}^4\overline{\text{He}}$ nuclei are consistent with the predictions from the various (equilibrium) thermal models (THERMUS [45], GSI [5,46,47] and SHARE [48–50]) with $T_{\text{chem}} = 156$ MeV, as shown in Fig. 3 for complete statistical thermal model fits using the available light flavour data measured by the ALICE Collaboration. The fits in Fig. 3 extend the simple exponential model (Fig. 2) by incorporating Boltzmann statistics and degeneracy factors for all particles. If instead of all listed

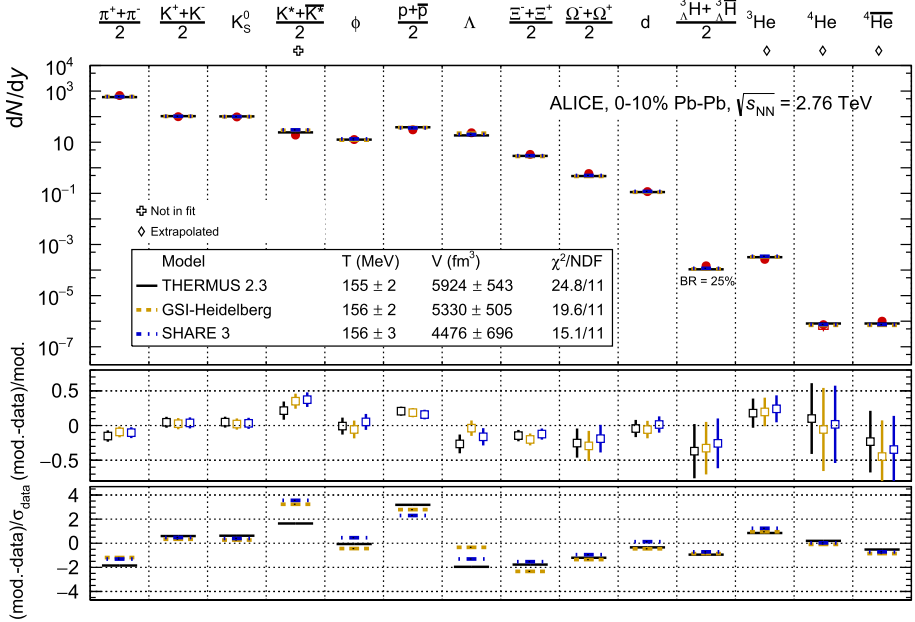


Fig. 3. Thermal model fits, with three different implementations, to the light flavour hadron yields in central (0–10%) Pb–Pb collisions at $\sqrt{s_{\text{NN}}} = 2.76 \text{ TeV}$. The data points are taken from [1,2,38,51–54] and details of the fits can be found in [10,11]. The upper panel shows the fit results together with the data, whereas the middle panel shows the difference between model and data normalised to the model value and the lower panel the difference between model and data normalised to the experimental uncertainties.

particles only nuclei (deuterons, ${}^3\text{He}$ and ${}^4\text{He}$ and ${}^4\overline{\text{He}}$) are considered for the fit, the resulting temperatures are $154 \pm 4 \text{ MeV}$. The pure measured yields for ${}^4\text{He}$ and ${}^4\overline{\text{He}}$ nuclei agree, depending on the model implementation, within the determined uncertainties with temperatures from 135 MeV to 177 MeV. Taken together these observations suggest that the relatively heavy ${}^4\text{He}$ and ${}^4\overline{\text{He}}$ nuclei are also produced statistically at the same temperature as the lighter particles.

5. Summary and conclusion

The ALICE Collaboration has measured the production yields of ${}^4\text{He}$ and ${}^4\overline{\text{He}}$ in central (0–10%) Pb–Pb collisions at $\sqrt{s_{\text{NN}}} = 2.76 \text{ TeV}$. The ratio of the two yields is consistent with unity and the results are in good agreement with the prediction of the statistical thermal model assuming the same temperature of 156 MeV as is obtained from the fit to the other light flavour hadrons.

Data gathered at the current beam energy of $\sqrt{s_{\text{NN}}} = 5.02 \text{ TeV}$ in Pb–Pb collisions at the LHC (*Run 2*) will improve the studies described in this letter thanks to an increase in statistics by a factor of about 3. Based on the pilot measurement presented here, we conclude that a precision study will be possible in the data taking period starting from 2021 (*Run 3* of the LHC), where about 5500 ${}^4\text{He}$ (${}^4\overline{\text{He}}$) particles are expected to be reconstructed [55]. This will allow for the measurement of the transverse-momentum spectra. As the unknown shape of the p_T distributions is one of the major sources of the systematic uncertainty, the measurement of the spectrum will decrease the systematic uncertainty of the measured yield. As a consequence the precision of

the ratio of ${}^4\overline{\text{He}}/{}^4\text{He}$ will be significantly improved. In addition, a mass difference measurement similar to what was done in [56] will be possible.

Acknowledgements

The ALICE Collaboration would like to thank all its engineers and technicians for their invaluable contributions to the construction of the experiment and the CERN accelerator teams for the outstanding performance of the LHC complex. The ALICE Collaboration gratefully acknowledges the resources and support provided by all Grid centres and the Worldwide LHC Computing Grid (WLCG) collaboration. The ALICE Collaboration acknowledges the following funding agencies for their support in building and running the ALICE detector: A.I. Alikhanyan National Science Laboratory (Yerevan Physics Institute) Foundation (ANSL), State Committee of Science and World Federation of Scientists (WFS), Armenia; Austrian Academy of Sciences and Nationalstiftung für Forschung, Technologie und Entwicklung, Austria; Ministry of Communications and High Technologies, National Nuclear Research Center, Azerbaijan; Conselho Nacional de Desenvolvimento Científico e Tecnológico (CNPq), Universidade Federal do Rio Grande do Sul (UFRGS), Financiadora de Estudos e Projetos (Finep) and Fundação de Amparo à Pesquisa do Estado de São Paulo (FAPESP), Brazil; Ministry of Science & Technology of China (MSTC), National Natural Science Foundation of China (NSFC) and Ministry of Education of China (MOEC), China; Ministry of Science, Education and Sports and Croatian Science Foundation, Croatia; Ministry of Education, Youth and Sports of the Czech Republic, Czech Republic; The Danish Council for Independent Research – Natural Sciences, the Carlsberg Foundation and Danish National Research Foundation (DNRF), Denmark; Helsinki Institute of Physics (HIP), Finland; Commissariat à l’Energie Atomique (CEA) and Institut National de Physique Nucléaire et de Physique des Particules (IN2P3) and Centre National de la Recherche Scientifique (CNRS), France; Bundesministerium für Bildung, Wissenschaft, Forschung und Technologie (BMBF) and GSI Helmholtzzentrum für Schwerionenforschung GmbH, Germany; General Secretariat for Research and Technology, Ministry of Education, Research and Religions, Greece; National Research, Development and Innovation Office, Hungary; Department of Atomic Energy, Government of India (DAE), Department of Science and Technology, Government of India (DST), University Grants Commission, Government of India (UGC) and Council of Scientific and Industrial Research (CSIR), India; Indonesian Institute of Science, Indonesia; Centro Fermi – Museo Storico della Fisica e Centro Studi e Ricerche Enrico Fermi and Istituto Nazionale di Fisica Nucleare (INFN), Italy; Institute for Innovative Science and Technology, Nagasaki Institute of Applied Science (IIST), Japan Society for the Promotion of Science (JSPS) KAKENHI and Japanese Ministry of Education, Culture, Sports, Science and Technology (MEXT), Japan; Consejo Nacional de Ciencia y Tecnología (CONACYT), through Fondo de Cooperación Internacional en Ciencia y Tecnología (FONCICYT) and Dirección General de Asuntos del Personal Académico (DGAPA), Mexico; Nederlandse Organisatie voor Wetenschappelijk Onderzoek (NWO), Netherlands; The Research Council of Norway, Norway; Commission on Science and Technology for Sustainable Development in the South (COMSATS), Pakistan; Pontificia Universidad Católica del Perú, Peru; Ministry of Science and Higher Education and National Science Centre, Poland; Korea Institute of Science and Technology Information and National Research Foundation of Korea (NRF), Republic of Korea; Ministry of Education and Scientific Research, Institute of Atomic Physics and Romanian National Agency for Science, Technology and Innovation, Romania; Joint Institute for Nuclear Research (JINR), Ministry of Education and Science of the Russian Federation and National Research Centre Kurchatov Institute, Russia;

Ministry of Education, Science, Research and Sport of the Slovak Republic, Slovakia; National Research Foundation of South Africa, South Africa; Centro de Aplicaciones Tecnológicas y Desarrollo Nuclear (CEADEN), Cubaenergía, Cuba, Ministerio de Ciencia e Innovacion and Centro de Investigaciones Energéticas, Medioambientales y Tecnológicas (CIEMAT), Spain; Swedish Research Council (VR) and Knut and Alice Wallenberg Foundation (KAW), Sweden; European Organization for Nuclear Research, Switzerland; National Science and Technology Development Agency (NSDTA), Suranaree University of Technology (SUT) and Office of the Higher Education Commission under NRU project of Thailand, Thailand; Turkish Atomic Energy Agency (TAEK), Turkey; National Academy of Sciences of Ukraine, Ukraine; Science and Technology Facilities Council (STFC), United Kingdom; National Science Foundation of the United States of America (NSF) and U.S. Department of Energy, Office of Nuclear Physics (DOE NP), United States of America.

References

- [1] ALICE Collaboration, J. Adam, et al., Production of light nuclei and anti-nuclei in pp and Pb–Pb collisions at LHC energies, *Phys. Rev. C* 93 (2016) 024917, <https://arxiv.org/abs/1506.08951v3>.
- [2] ALICE Collaboration, J. Adam, et al., ${}^3_{\Lambda}\text{H}$ and ${}^3_{\Lambda}\bar{\text{H}}$ production in Pb–Pb collisions at $\sqrt{s_{\text{NN}}} = 2.76$ TeV, *Phys. Lett. B* 754 (2016) 360, <https://arxiv.org/abs/1506.08453v2>.
- [3] P. Braun-Munzinger, J. Stachel, Production of strange clusters and strange matter in nucleus–nucleus collisions at the AGS, *J. Phys. G* 21 (1995) L17, <https://arxiv.org/abs/nucl-th/9412035v1>.
- [4] P. Braun-Munzinger, J. Stachel, Particle ratios, equilibration and the QCD phase boundary, *J. Phys. G* 28 (2002) 1971, <https://arxiv.org/abs/nucl-th/0112051v1>.
- [5] A. Andronic, P. Braun-Munzinger, J. Stachel, H. Stöcker, Production of light nuclei, hypernuclei and their antiparticles in relativistic nuclear collisions, *Phys. Lett. B* 697 (2011) 203, <https://arxiv.org/abs/1010.2995v2>.
- [6] J. Cleymans, S. Kabana, I. Kraus, H. Oeschler, K. Redlich, N. Sharma, Antimatter production in proton–proton and heavy-ion collisions at ultrarelativistic energies, *Phys. Rev. C* 84 (2011) 054916, <https://arxiv.org/abs/1105.3719v1>.
- [7] A. Andronic, P. Braun-Munzinger, K. Redlich, J. Stachel, The statistical model in Pb–Pb collisions at the LHC, *Nucl. Phys. A* 904 (2013) 535c, <https://arxiv.org/abs/1210.7724v1>.
- [8] J. Stachel, A. Andronic, P. Braun-Munzinger, K. Redlich, Confronting LHC data with the statistical hadronization model, *J. Phys. Conf. Ser.* 509 (2014) 012019, <https://arxiv.org/abs/1311.4662v1>.
- [9] J. Steinheimer, K. Gudima, A. Botvina, I. Mishustin, M. Bleicher, H. Stöcker, Hypernuclei, dibaryon and antinuclei production in high energy heavy ion collisions: thermal production vs. coalescence, *Phys. Lett. B* 714 (2012) 85, <https://arxiv.org/abs/1203.2547v2>.
- [10] M. Floris, Hadron yields and the phase diagram of strongly interacting matter, *Nucl. Phys. A* 931 (2014) 103, <https://arxiv.org/abs/1408.6403v3>.
- [11] A. Andronic, P. Braun-Munzinger, K. Redlich, J. Stachel, Hadron yields, the chemical freeze-out and the QCD phase diagram, *J. Phys. Conf. Ser.* 779 (2017) 012012, <https://arxiv.org/abs/1611.01347v2>.
- [12] STAR Collaboration, H. Agakishiev, et al., Observation of the antimatter helium-4 nucleus, *Nature* 473 (2011) 353, <https://arxiv.org/abs/1103.3312v2>, Erratum: *Nature* 475 (2011) 412.
- [13] P. Braun-Munzinger, J. Stachel, The quest for the quark–gluon plasma, *Nature* 448 (2007) 302.
- [14] H. Sato, K. Yazaki, On the coalescence model for high energy nuclear reactions, *Phys. Lett. B* 98 (1981) 153.
- [15] R. Hagedorn, Deuteron production in high-energy collisions, *Phys. Rev. Lett.* 5 (1960) 276–277.
- [16] S.T. Butler, C.A. Pearson, Deuterons from high-energy proton bombardment of matter, *Phys. Rev. Lett.* 7 (Jul 1961) 69–71, <https://doi.org/10.1103/PhysRevLett.7.69>.
- [17] S.T. Butler, C.A. Pearson, Deuterons from high-energy proton bombardment of matter, *Phys. Rev.* 129 (Jan 1963) 836–842, <https://doi.org/10.1103/PhysRev.129.836>.
- [18] J.L. Nagle, B.S. Kumar, D. Kusnezov, H. Sorge, R. Mattiello, Coalescence of deuterons in relativistic heavy ion collisions, *Phys. Rev. C* 53 (1996) 367–376.
- [19] R. Scheibl, U.W. Heinz, Coalescence and flow in ultrarelativistic heavy ion collisions, *Phys. Rev. C* 59 (1999) 1585–1602, arXiv:nucl-th/9809022.
- [20] Y. Oh, Z.-W. Lin, C.M. Ko, Deuteron production and elliptic flow in relativistic heavy ion collisions, *Phys. Rev. C* 80 (Dec 2009) 064902, <https://doi.org/10.1103/PhysRevC.80.064902>.

- [21] L. Zhu, C.M. Ko, X. Yin, Light (anti-)nuclei production and flow in relativistic heavy-ion collisions, Phys. Rev. C 92 (6) (2015) 064911, arXiv:1510.03568 [nucl-th].
- [22] X. Yin, C.M. Ko, Y. Sun, L. Zhu, Elliptic flow of light nuclei, Phys. Rev. C 95 (5) (2017) 054913, arXiv:1703.09383 [nucl-th].
- [23] L. Zhu, H. Zheng, C.M. Ko, Y. Sun, Light nuclei production in Pb+Pb collisions at $\sqrt{s_{\text{NN}}} = 2.76$ TeV, arXiv:1710.05139 [nucl-th].
- [24] A.S. Botvina, J. Steinheimer, M. Bleicher, Formation of exotic baryon clusters in ultra-relativistic heavy-ion collisions, Phys. Rev. C 96 (1) (2017) 014913, arXiv:1706.08335 [nucl-th].
- [25] K.-J. Sun, L.-W. Chen, An analytical coalescence formula for particle production in relativistic heavy-ion collisions, arXiv:1701.01935 [nucl-th].
- [26] J. Alme, et al., The ALICE TPC, a large 3-dimensional tracking device with fast readout for ultra-high multiplicity events, Nucl. Instrum. Methods A 622 (2010) 316, <https://arxiv.org/abs/1001.1950v1>.
- [27] A. Akindinov, et al., Performance of the ALICE Time-Of-Flight detector at the LHC, Eur. Phys. J. Plus 128 (2013) 44.
- [28] ALICE Collaboration, K. Aamodt, et al., Centrality dependence of the charged-particle multiplicity density at midrapidity in Pb–Pb collisions at $\sqrt{s_{\text{NN}}} = 2.76$ TeV, Phys. Rev. Lett. 106 (2011) 032301, <https://arxiv.org/abs/1012.1657v2>.
- [29] ALICE Collaboration, B. Abelev, et al., Centrality determination of Pb–Pb collisions at $\sqrt{s_{\text{NN}}} = 2.76$ TeV with ALICE, Phys. Rev. C 88 (2013) 044909, <https://arxiv.org/abs/1301.4361v3>.
- [30] ALICE Collaboration, K. Aamodt, et al., Alignment of the ALICE Inner Tracking System with cosmic-ray tracks, J. Instrum. 5 (2010) P03003, <https://arxiv.org/abs/1001.0502v3>.
- [31] ALICE Collaboration, The ALICE definition of primary particles, <https://cds.cern.ch/record/2270008>.
- [32] ALICE Collaboration, K. Aamodt, et al., The ALICE experiment at the CERN LHC, J. Instrum. 3 (2008) S08002.
- [33] ALICE Collaboration, B. Abelev, et al., Performance of the ALICE experiment at the CERN LHC, Int. J. Mod. Phys. A 29 (2014) 1430044, <https://arxiv.org/abs/1402.4476v4>.
- [34] H. Bethe, Bremsformel für Elektronen relativistischer Geschwindigkeit, Z. Phys. 76 (1932) 293.
- [35] F. Bloch, Zur Bremsung rasch bewegter Teilchen beim Durchgang durch Materie, Ann. Phys. 408 (1933) 285.
- [36] E. Schnedermann, J. Sollfrank, U.W. Heinz, Thermal phenomenology of hadrons from 200-A/GeV S+S collisions, Phys. Rev. C 48 (1993) 2462, <https://arxiv.org/abs/nucl-th/9307020v1>.
- [37] ALICE Collaboration, B. Abelev, et al., Pion, kaon, and proton production in central Pb–Pb collisions at $\sqrt{s_{\text{NN}}} = 2.76$ TeV, Phys. Rev. Lett. 109 (2012) 252301, <https://arxiv.org/abs/1208.1974v3>.
- [38] ALICE Collaboration, B. Abelev, et al., Centrality dependence of π , K, p production in Pb–Pb collisions at $\sqrt{s_{\text{NN}}} = 2.76$ TeV, Phys. Rev. C 88 (2013) 044910, <https://arxiv.org/abs/1303.0737v3>.
- [39] ALICE Collaboration, J. Adam, et al., Search for weakly decaying $\Lambda\bar{n}$ and $\Lambda\Lambda$ exotic bound states in central Pb–Pb collisions at $\sqrt{s_{\text{NN}}} = 2.76$ TeV, Phys. Lett. B 752 (2016) 267, <https://arxiv.org/abs/1506.07499v2>.
- [40] R. Brun, F. Carminati, S. Giani, GEANT Detector Description and Simulation Tool, CERN-W5013, CERN-W-5013, 1994.
- [41] S. Agostinelli, et al., GEANT 4: a simulation toolkit, Nucl. Instrum. Methods A 506 (2003) 250.
- [42] V. Uzhinsky, et al., Antinucleus–nucleus cross sections implemented in geant4, Phys. Lett. B 705 (2011) 235.
- [43] A.A. Moiseev, J.F. Ormes, Inelastic cross section for antihelium on nuclei: an empirical formula for use in the experiments to search for cosmic antimatter, Astropart. Phys. 6 (1997) 379.
- [44] V.V. Abramov, et al., Production of deuterons and antideuterons with large pt in pp and pA collisions at 70 GeV, Yad. Fiz. 45 (1987) 1362.
- [45] S. Wheaton, J. Cleymans, M. Hauer, THERMUS – a thermal model package for ROOT, Comput. Phys. Commun. 180 (2009) 84, <https://arxiv.org/abs/hep-ph/0407174v2>.
- [46] A. Andronic, P. Braun-Munzinger, J. Stachel, Thermal hadron production in relativistic nuclear collisions: the hadron mass spectrum, the horn, and the QCD phase transition, Phys. Lett. B 673 (2009) 142, <https://arxiv.org/abs/0812.1186v3>, Erratum: Phys. Lett. B 678 (2009) 516.
- [47] A. Andronic, P. Braun-Munzinger, K. Redlich, J. Stachel, Decoding the phase structure of QCD via particle production at high energy, arXiv:1710.09425 [nucl-th].
- [48] G. Torrieri, S. Steinke, W. Broniowski, W. Florkowski, J. Letessier, J. Rafelski, SHARE: statistical hadronization with resonances, Comput. Phys. Commun. 167 (2005) 229, <https://arxiv.org/abs/nucl-th/0404083v2>.
- [49] G. Torrieri, S. Jeon, J. Letessier, J. Rafelski, SHAREv2: fluctuations and a comprehensive treatment of decay feed-down, Comput. Phys. Commun. 175 (2006) 635, <https://arxiv.org/abs/nucl-th/0603026v2>.
- [50] M. Petran, J. Letessier, J. Rafelski, G. Torrieri, SHARE with CHARM, Comput. Phys. Commun. 185 (2014) 2056, <https://arxiv.org/abs/1310.5108v2>.

- [51] ALICE Collaboration, B. Abelev, et al., K_s^0 and Λ production in Pb–Pb collisions at $\sqrt{s_{\text{NN}}} = 2.76$ TeV, Phys. Rev. Lett. 111 (2013) 222301, <https://arxiv.org/abs/1307.5530v2>.
- [52] ALICE Collaboration, B. Abelev, et al., Multi-strange baryon production at mid-rapidity in Pb–Pb collisions at $\sqrt{s_{\text{NN}}} = 2.76$ TeV, Phys. Lett. B 728 (2014) 216, <https://arxiv.org/abs/1307.5543v3>.
- [53] ALICE Collaboration, B. Abelev, et al., $K^*(892)^0$ and $\phi(1020)$ production in Pb–Pb collisions at $\sqrt{s_{\text{NN}}} = 2.76$ TeV, Phys. Rev. C 91 (2015) 024609, <https://arxiv.org/abs/1404.0495v3>.
- [54] ALICE Collaboration, J. Adam, et al., $K^*(892)^0$ and $\phi(1020)$ meson production at high transverse momentum in pp and Pb–Pb collisions at $\sqrt{s_{\text{NN}}} = 2.76$ TeV, Phys. Rev. C 95 (2017) 064606, arXiv:1702.00555 [nucl-ex].
- [55] ALICE Collaboration, B. Abelev, et al., Upgrade of the ALICE experiment: letter of intent, J. Phys. G, Nucl. Part. Phys. 41 (2014) 087001.
- [56] ALICE Collaboration, J. Adam, et al., Precision measurement of the mass difference between light nuclei and anti-nuclei, Nat. Phys. 11 (2015) 811, <https://arxiv.org/abs/1508.03986v1>.

ALICE Collaboration

S. Acharya ¹³⁷, D. Adamová ⁹⁴, J. Adolfsson ³⁴, M.M. Aggarwal ⁹⁹,
 G. Aglieri Rinella ³⁵, M. Agnello ³¹, N. Agrawal ⁴⁸, Z. Ahammed ¹³⁷,
 S.U. Ahn ⁷⁹, S. Aiola ¹⁴¹, A. Akindinov ⁶⁴, M. Al-Turany ¹⁰⁶,
 S.N. Alam ¹³⁷, D.S.D. Albuquerque ¹²², D. Aleksandrov ⁹⁰,
 B. Alessandro ⁵⁸, R. Alfaro Molina ⁷⁴, Y. Ali ¹⁵, A. Alici ^{12,53,27}, A. Alkin ³,
 J. Alme ²², T. Alt ⁷⁰, L. Altenkamper ²², I. Altsybeev ¹³⁶,
 C. Alves Garcia Prado ¹²¹, C. Andrei ⁸⁷, D. Andreou ³⁵, H.A. Andrews ¹¹⁰,
 A. Andronic ¹⁰⁶, V. Anguelov ¹⁰⁴, C. Anson ⁹⁷, T. Antićić ¹⁰⁷, F. Antinori ⁵⁶,
 P. Antonioli ⁵³, L. Aphecetche ¹¹⁴, H. Appelshäuser ⁷⁰, S. Arcelli ²⁷,
 R. Arnaldi ⁵⁸, O.W. Arnold ^{105,36}, I.C. Arsene ²¹, M. Arslanbekov ¹⁰⁴,
 B. Audurier ¹¹⁴, A. Augustinus ³⁵, R. Averbeck ¹⁰⁶, M.D. Azmi ¹⁷,
 A. Badalà ⁵⁵, Y.W. Baek ^{60,78}, S. Bagnasco ⁵⁸, R. Bailhache ⁷⁰, R. Bala ¹⁰¹,
 A. Baldissari ⁷⁵, M. Ball ⁴⁵, R.C. Baral ^{67,88}, A.M. Barbano ²⁶,
 R. Barbera ²⁸, F. Barile ³³, L. Barioglio ²⁶, G.G. Barnaföldi ¹⁴⁰,
 L.S. Barnby ⁹³, V. Barret ¹³¹, P. Bartalini ⁷, K. Barth ³⁵, E. Bartsch ⁷⁰,
 N. Bastid ¹³¹, S. Basu ¹³⁹, G. Batigne ¹¹⁴, B. Batyunya ⁷⁷, P.C. Batzing ²¹,
 J.L. Bazo Alba ¹¹¹, I.G. Bearden ⁹¹, H. Beck ¹⁰⁴, C. Bedda ⁶³,
 N.K. Behera ⁶⁰, I. Belikov ¹³³, F. Bellini ^{27,35}, H. Bello Martinez ²,
 R. Bellwied ¹²⁴, L.G.E. Beltran ¹²⁰, V. Belyaev ⁸³, G. Bencedi ¹⁴⁰,
 S. Beole ²⁶, A. Bercuci ⁸⁷, Y. Berdnikov ⁹⁶, D. Berenyi ¹⁴⁰, R.A. Bertens ¹²⁷,
 D. Berzana ³⁵, L. Betev ³⁵, A. Bhasin ¹⁰¹, I.R. Bhat ¹⁰¹, B. Bhattacharjee ⁴⁴,
 J. Bhom ¹¹⁸, A. Bianchi ²⁶, L. Bianchi ¹²⁴, N. Bianchi ⁵¹, C. Bianchin ¹³⁹,
 J. Bielčík ³⁹, J. Bielčíková ⁹⁴, A. Bilandžić ^{36,105}, G. Biro ¹⁴⁰, R. Biswas ⁴,
 S. Biswas ⁴, J.T. Blair ¹¹⁹, D. Blau ⁹⁰, C. Blume ⁷⁰, G. Boca ¹³⁴, F. Bock ³⁵,
 A. Bogdanov ⁸³, L. Boldizsár ¹⁴⁰, M. Bombara ⁴⁰, G. Bonomi ¹³⁵,
 M. Bonora ³⁵, J. Book ⁷⁰, H. Borel ⁷⁵, A. Borissov ^{104,19}, M. Borri ¹²⁶,
 E. Botta ²⁶, C. Bourjau ⁹¹, L. Bratrud ⁷⁰, P. Braun-Munzinger ¹⁰⁶,

M. Bregant ¹²¹, T.A. Broker ⁷⁰, M. Broz ³⁹, E.J. Brucken ⁴⁶, E. Bruna ⁵⁸,
 G.E. Bruno ^{35,33}, D. Budnikov ¹⁰⁸, H. Buesching ⁷⁰, S. Bufalino ³¹,
 P. Buhler ¹¹³, P. Buncic ³⁵, O. Busch ¹³⁰, Z. Buthelezi ⁷⁶, J.B. Butt ¹⁵,
 J.T. Buxton ¹⁸, J. Cabala ¹¹⁶, D. Caffarri ^{35,92}, H. Caines ¹⁴¹, A. Caliva ^{63,106},
 E. Calvo Villar ¹¹¹, P. Camerini ²⁵, A.A. Capon ¹¹³, F. Carena ³⁵,
 W. Carena ³⁵, F. Carnesecchi ^{27,12}, J. Castillo Castellanos ⁷⁵, A.J. Castro ¹²⁷,
 E.A.R. Casula ⁵⁴, C. Ceballos Sanchez ⁹, S. Chandra ¹³⁷, B. Chang ¹²⁵,
 W. Chang ⁷, S. Chapelard ³⁵, M. Chartier ¹²⁶, S. Chattopadhyay ¹³⁷,
 S. Chattopadhyay ¹⁰⁹, A. Chauvin ^{36,105}, C. Cheshkov ¹³², B. Cheynis ¹³²,
 V. Chibante Barroso ³⁵, D.D. Chinellato ¹²², S. Cho ⁶⁰, P. Chochula ³⁵,
 M. Chojnacki ⁹¹, S. Choudhury ¹³⁷, T. Chowdhury ¹³¹, P. Christakoglou ⁹²,
 C.H. Christensen ⁹¹, P. Christiansen ³⁴, T. Chujo ¹³⁰, S.U. Chung ¹⁹,
 C. Cicalo ⁵⁴, L. Cifarelli ^{12,27}, F. Cindolo ⁵³, J. Cleymans ¹⁰⁰,
 F. Colamaria ^{52,33}, D. Colella ^{35,52,65}, A. Collu ⁸², M. Colocci ²⁷,
 M. Concas ^{58,ii}, G. Conesa Balbastre ⁸¹, Z. Conesa del Valle ⁶¹,
 J.G. Contreras ³⁹, T.M. Cormier ⁹⁵, Y. Corrales Morales ⁵⁸,
 I. Cortés Maldonado ², P. Cortese ³², M.R. Cosentino ¹²³, F. Costa ³⁵,
 S. Costanza ¹³⁴, J. Crkovská ⁶¹, P. Crochet ¹³¹, E. Cuautle ⁷²,
 L. Cunqueiro ^{95,71}, T. Dahms ^{36,105}, A. Dainese ⁵⁶, M.C. Danisch ¹⁰⁴,
 A. Danu ⁶⁸, D. Das ¹⁰⁹, I. Das ¹⁰⁹, S. Das ⁴, A. Dash ⁸⁸, S. Dash ⁴⁸, S. De ⁴⁹,
 A. De Caro ³⁰, G. de Cataldo ⁵², C. de Conti ¹²¹, J. de Cuveland ⁴²,
 A. De Falco ²⁴, D. De Gruttola ^{30,12}, N. De Marco ⁵⁸, S. De Pasquale ³⁰,
 R.D. De Souza ¹²², H.F. Degenhardt ¹²¹, A. Deisting ^{106,104}, A. Deloff ⁸⁶,
 C. Deplano ⁹², P. Dhankher ⁴⁸, D. Di Bari ³³, A. Di Mauro ³⁵,
 P. Di Nezza ⁵¹, B. Di Ruzza ⁵⁶, M.A. Diaz Corchero ¹⁰, T. Dietel ¹⁰⁰,
 P. Dillenseger ⁷⁰, Y. Ding ⁷, R. Divià ³⁵, Ø. Djupsland ²², A. Dobrin ³⁵,
 D. Domenicis Gimenez ¹²¹, B. Dönigus ⁷⁰, O. Dordic ²¹,
 L.V.R. Doremalen ⁶³, A.K. Dubey ¹³⁷, A. Dubla ¹⁰⁶, L. Ducroux ¹³²,
 S. Dudi ⁹⁹, A.K. Duggal ⁹⁹, M. Dukhishyam ⁸⁸, P. Dupieux ¹³¹,
 R.J. Ehlers ¹⁴¹, D. Elia ⁵², E. Endress ¹¹¹, H. Engel ⁶⁹, E. Epple ¹⁴¹,
 B. Erazmus ¹¹⁴, F. Erhardt ⁹⁸, B. Espagnon ⁶¹, G. Eulisse ³⁵, J. Eum ¹⁹,
 D. Evans ¹¹⁰, S. Evdokimov ¹¹², L. Fabbietti ^{105,36}, J. Faivre ⁸¹,
 A. Fantoni ⁵¹, M. Fasel ⁹⁵, L. Feldkamp ⁷¹, A. Feliciello ⁵⁸, G. Feofilov ¹³⁶,
 A. Fernández Téllez ², E.G. Ferreiro ¹⁶, A. Ferretti ²⁶, A. Festanti ^{29,35},
 V.J.G. Feuillard ^{75,131}, J. Figiel ¹¹⁸, M.A.S. Figueiredo ¹²¹, S. Filchagin ¹⁰⁸,
 D. Finogeev ⁶², F.M. Fionda ^{22,24}, M. Floris ³⁵, S. Foertsch ⁷⁶, P. Foka ¹⁰⁶,
 S. Fokin ⁹⁰, E. Fragiocomo ⁵⁹, A. Francescon ³⁵, A. Francisco ¹¹⁴,

- U. Frankenfeld ¹⁰⁶, G.G. Fronze ²⁶, U. Fuchs ³⁵, C. Furget ⁸¹, A. Furs ⁶²,
 M. Fusco Girard ³⁰, J.J. Gaardhøje ⁹¹, M. Gagliardi ²⁶, A.M. Gago ¹¹¹,
 K. Gajdosova ⁹¹, M. Gallio ²⁶, C.D. Galvan ¹²⁰, P. Ganoti ⁸⁵,
 C. Garabatos ¹⁰⁶, E. Garcia-Solis ¹³, K. Garg ²⁸, C. Gargiulo ³⁵,
 P. Gasik ^{105,36}, E.F. Gauger ¹¹⁹, M.B. Gay Ducati ⁷³, M. Germain ¹¹⁴,
 J. Ghosh ¹⁰⁹, P. Ghosh ¹³⁷, S.K. Ghosh ⁴, P. Gianotti ⁵¹,
 P. Giubellino ^{35,106,58}, P. Giubilato ²⁹, E. Gladysz-Dziadus ¹¹⁸, P. Glässel ¹⁰⁴,
 D.M. Goméz Coral ⁷⁴, A. Gomez Ramirez ⁶⁹, A.S. Gonzalez ³⁵,
 V. Gonzalez ¹⁰, P. González-Zamora ^{10,2}, S. Gorbunov ⁴², L. Görlich ¹¹⁸,
 S. Gotovac ¹¹⁷, V. Grabski ⁷⁴, L.K. Graczykowski ¹³⁸, K.L. Graham ¹¹⁰,
 L. Greiner ⁸², A. Grelli ⁶³, C. Grigoras ³⁵, V. Grigoriev ⁸³, A. Grigoryan ¹,
 S. Grigoryan ⁷⁷, J.M. Gronefeld ¹⁰⁶, F. Grossa ³¹, J.F. Grosse-Oetringhaus ³⁵,
 R. Grosso ¹⁰⁶, F. Guber ⁶², R. Guernane ⁸¹, B. Guerzoni ²⁷,
 K. Gulbrandsen ⁹¹, T. Gunji ¹²⁹, A. Gupta ¹⁰¹, R. Gupta ¹⁰¹, I.B. Guzman ²,
 R. Haake ³⁵, C. Hadjidakis ⁶¹, H. Hamagaki ⁸⁴, G. Hamar ¹⁴⁰,
 J.C. Hamon ¹³³, M.R. Haque ⁶³, J.W. Harris ¹⁴¹, A. Harton ¹³, H. Hassan ⁸¹,
 D. Hatzifotiadou ^{12,53}, S. Hayashi ¹²⁹, S.T. Heckel ⁷⁰, E. Hellbär ⁷⁰,
 H. Helstrup ³⁷, A. Herghelegiu ⁸⁷, E.G. Hernandez ², G. Herrera Corral ¹¹,
 F. Herrmann ⁷¹, B.A. Hess ¹⁰³, K.F. Hetland ³⁷, H. Hillemanns ³⁵,
 C. Hills ¹²⁶, B. Hippolyte ¹³³, B. Hohlweyer ¹⁰⁵, D. Horak ³⁹,
 S. Hornung ¹⁰⁶, R. Hosokawa ^{81,130}, P. Hristov ³⁵, C. Hughes ¹²⁷,
 T.J. Humanic ¹⁸, N. Hussain ⁴⁴, T. Hussain ¹⁷, D. Hutter ⁴², D.S. Hwang ²⁰,
 S.A. Iga Buitron ⁷², R. Ilkaev ¹⁰⁸, M. Inaba ¹³⁰, M. Ippolitov ^{83,90},
 M.S. Islam ¹⁰⁹, M. Ivanov ¹⁰⁶, V. Ivanov ⁹⁶, V. Izucheev ¹¹², B. Jacak ⁸²,
 N. Jacazio ²⁷, P.M. Jacobs ⁸², M.B. Jadhav ⁴⁸, S. Jadlovska ¹¹⁶,
 J. Jadlovsky ¹¹⁶, S. Jaelani ⁶³, C. Jahnke ³⁶, M.J. Jakubowska ¹³⁸,
 M.A. Janik ¹³⁸, P.H.S.Y. Jayarathna ¹²⁴, C. Jena ⁸⁸, M. Jercic ⁹⁸,
 R.T. Jimenez Bustamante ¹⁰⁶, P.G. Jones ¹¹⁰, A. Jusko ¹¹⁰, P. Kalinak ⁶⁵,
 A. Kalweit ³⁵, J.H. Kang ¹⁴², V. Kaplin ⁸³, S. Kar ¹³⁷, A. Karasu Uysal ⁸⁰,
 O. Karavichev ⁶², T. Karavicheva ⁶², L. Karayan ^{106,104}, P. Karczmarczyk ³⁵,
 E. Karpechev ⁶², U. Kebschull ⁶⁹, R. Keidel ¹⁴³, D.L.D. Keijdener ⁶³,
 M. Keil ³⁵, B. Ketzer ⁴⁵, Z. Khabanova ⁹², P. Khan ¹⁰⁹, S.A. Khan ¹³⁷,
 A. Khanzadeev ⁹⁶, Y. Kharlov ¹¹², A. Khatun ¹⁷, A. Khuntia ⁴⁹,
 M.M. Kielbowicz ¹¹⁸, B. Kileng ³⁷, B. Kim ¹³⁰, D. Kim ¹⁴², D.J. Kim ¹²⁵,
 H. Kim ¹⁴², J.S. Kim ⁴³, J. Kim ¹⁰⁴, M. Kim ⁶⁰, S. Kim ²⁰, T. Kim ¹⁴²,
 S. Kirsch ⁴², I. Kisiel ⁴², S. Kiselev ⁶⁴, A. Kisiel ¹³⁸, G. Kiss ¹⁴⁰, J.L. Klay ⁶,
 C. Klein ⁷⁰, J. Klein ³⁵, C. Klein-Bösing ⁷¹, S. Klewin ¹⁰⁴, A. Kluge ³⁵,

- M.L. Knichel ^{104,35}, A.G. Knospe ¹²⁴, C. Kobdaj ¹¹⁵, M. Kofarago ¹⁴⁰,
 M.K. Köhler ¹⁰⁴, T. Kollegger ¹⁰⁶, V. Kondratiev ¹³⁶, N. Kondratyeva ⁸³,
 E. Kondratyuk ¹¹², A. Konevskikh ⁶², M. Konyushikhin ¹³⁹, M. Kopcik ¹¹⁶,
 M. Kour ¹⁰¹, C. Kouzinopoulos ³⁵, O. Kovalenko ⁸⁶, V. Kovalenko ¹³⁶,
 M. Kowalski ¹¹⁸, G. Koyithatta Meethaleveedu ⁴⁸, I. Králik ⁶⁵,
 A. Kravčáková ⁴⁰, L. Kreis ¹⁰⁶, M. Krivda ^{110,65}, F. Krizek ⁹⁴, E. Kryshen ⁹⁶,
 M. Krzewicki ⁴², A.M. Kubera ¹⁸, V. Kučera ⁹⁴, C. Kuhn ¹³³, P.G. Kuijer ⁹²,
 A. Kumar ¹⁰¹, J. Kumar ⁴⁸, L. Kumar ⁹⁹, S. Kumar ⁴⁸, S. Kundu ⁸⁸,
 P. Kurashvili ⁸⁶, A. Kurepin ⁶², A.B. Kurepin ⁶², A. Kuryakin ¹⁰⁸,
 S. Kushpil ⁹⁴, M.J. Kweon ⁶⁰, Y. Kwon ¹⁴², S.L. La Pointe ⁴²,
 P. La Rocca ²⁸, C. Lagana Fernandes ¹²¹, Y.S. Lai ⁸², I. Lakomov ³⁵,
 R. Langoy ⁴¹, K. Lapidus ¹⁴¹, C. Lara ⁶⁹, A. Lardeux ²¹, A. Lattuca ²⁶,
 E. Laudi ³⁵, R. Lavicka ³⁹, R. Lea ²⁵, L. Leardini ¹⁰⁴, S. Lee ¹⁴², F. Lehas ⁹²,
 S. Lehner ¹¹³, J. Lehrbach ⁴², R.C. Lemmon ⁹³, E. Leogrande ⁶³,
 I. León Monzón ¹²⁰, P. Lévai ¹⁴⁰, X. Li ¹⁴, J. Lien ⁴¹, R. Lietava ¹¹⁰,
 B. Lim ¹⁹, S. Lindal ²¹, V. Lindenstruth ⁴², S.W. Lindsay ¹²⁶,
 C. Lippmann ¹⁰⁶, M.A. Lisa ¹⁸, V. Litichevskyi ⁴⁶, W.J. Llope ¹³⁹,
 D.F. Lodato ⁶³, P.I. Loenne ²², V. Loginov ⁸³, C. Loizides ^{95,82},
 P. Loncar ¹¹⁷, X. Lopez ¹³¹, E. López Torres ⁹, A. Lowe ¹⁴⁰, P. Luettig ⁷⁰,
 J.R. Luhder ⁷¹, M. Lunardon ²⁹, G. Luparello ^{59,25}, M. Lupi ³⁵,
 T.H. Lutz ¹⁴¹, A. Maevskaia ⁶², M. Mager ³⁵, S.M. Mahmood ²¹,
 A. Maire ¹³³, R.D. Majka ¹⁴¹, M. Malaev ⁹⁶, L. Malinina ^{77,iii},
 D. Mal'Kevich ⁶⁴, P. Malzacher ¹⁰⁶, A. Mamonov ¹⁰⁸, V. Manko ⁹⁰,
 F. Manso ¹³¹, V. Manzari ⁵², Y. Mao ⁷, M. Marchisone ^{132,76,128}, J. Mareš ⁶⁶,
 G.V. Margagliotti ²⁵, A. Margotti ⁵³, J. Margutti ⁶³, A. Marín ¹⁰⁶,
 C. Markert ¹¹⁹, M. Marquard ⁷⁰, N.A. Martin ¹⁰⁶, P. Martinengo ³⁵,
 J.A.L. Martinez ⁶⁹, M.I. Martínez ², G. Martínez García ¹¹⁴,
 M. Martinez Pedreira ³⁵, S. Masciocchi ¹⁰⁶, M. Masera ²⁶, A. Masoni ⁵⁴,
 E. Masson ¹¹⁴, A. Mastroserio ⁵², A.M. Mathis ^{105,36}, P.F.T. Matuoka ¹²¹,
 A. Matyja ¹²⁷, C. Mayer ¹¹⁸, J. Mazer ¹²⁷, M. Mazzilli ³³, M.A. Mazzoni ⁵⁷,
 F. Meddi ²³, Y. Melikyan ⁸³, A. Menchaca-Rocha ⁷⁴, E. Meninno ³⁰,
 J. Mercado Pérez ¹⁰⁴, M. Meres ³⁸, S. Mhlanga ¹⁰⁰, Y. Miake ¹³⁰,
 M.M. Mieskolainen ⁴⁶, D.L. Mihaylov ¹⁰⁵, K. Mikhaylov ^{77,64},
 A. Mischke ⁶³, A.N. Mishra ⁴⁹, D. Miśkowiec ¹⁰⁶, J. Mitra ¹³⁷, C.M. Mitu ⁶⁸,
 N. Mohammadi ⁶³, A.P. Mohanty ⁶³, B. Mohanty ⁸⁸, M. Mohisin Khan ^{17,iv},
 E. Montes ¹⁰, D.A. Moreira De Godoy ⁷¹, L.A.P. Moreno ², S. Moretto ²⁹,
 A. Morreale ¹¹⁴, A. Morsch ³⁵, V. Muccifora ⁵¹, E. Mudnic ¹¹⁷,

- D. Mühlheim ⁷¹, S. Muhuri ¹³⁷, J.D. Mulligan ¹⁴¹, M.G. Munhoz ¹²¹,
 K. Münnig ⁴⁵, R.H. Munzer ⁷⁰, H. Murakami ¹²⁹, S. Murray ⁷⁶,
 L. Musa ³⁵, J. Musinsky ⁶⁵, C.J. Myers ¹²⁴, J.W. Myrcha ¹³⁸, D. Nag ⁴,
 B. Naik ⁴⁸, R. Nair ⁸⁶, B.K. Nandi ⁴⁸, R. Nania ^{12,53}, E. Nappi ⁵²,
 A. Narayan ⁴⁸, M.U. Naru ¹⁵, H. Natal da Luz ¹²¹, C. Nattrass ¹²⁷,
 S.R. Navarro ², K. Nayak ⁸⁸, R. Nayak ⁴⁸, T.K. Nayak ¹³⁷, S. Nazarenko ¹⁰⁸,
 R.A. Negrao De Oliveira ^{70,35}, L. Nellen ⁷², S.V. Nesbo ³⁷, F. Ng ¹²⁴,
 M. Nicassio ¹⁰⁶, M. Niculescu ⁶⁸, J. Niedziela ^{35,138}, B.S. Nielsen ⁹¹,
 S. Nikolaev ⁹⁰, S. Nikulin ⁹⁰, V. Nikulin ⁹⁶, F. Noferini ^{12,53},
 P. Nomokonov ⁷⁷, G. Nooren ⁶³, J.C.C. Noris ², J. Norman ¹²⁶,
 A. Nyanin ⁹⁰, J. Nystrand ²², H. Oeschler ^{19,104,i}, H. Oh ¹⁴², A. Ohlson ¹⁰⁴,
 T. Okubo ⁴⁷, L. Olah ¹⁴⁰, J. Oleniacz ¹³⁸, A.C. Oliveira Da Silva ¹²¹,
 M.H. Oliver ¹⁴¹, J. Onderwaater ¹⁰⁶, C. Oppedisano ⁵⁸, R. Orava ⁴⁶,
 M. Oravec ¹¹⁶, A. Ortiz Velasquez ⁷², A. Oskarsson ³⁴, J. Otwinowski ¹¹⁸,
 K. Oyama ⁸⁴, Y. Pachmayer ¹⁰⁴, V. Pacik ⁹¹, D. Pagano ¹³⁵, G. Paić ⁷²,
 P. Palni ⁷, J. Pan ¹³⁹, A.K. Pandey ⁴⁸, S. Panebianco ⁷⁵, V. Papikyan ¹,
 P. Pareek ⁴⁹, J. Park ⁶⁰, S. Parmar ⁹⁹, A. Passfeld ⁷¹, S.P. Pathak ¹²⁴,
 R.N. Patra ¹³⁷, B. Paul ⁵⁸, H. Pei ⁷, T. Peitzmann ⁶³, X. Peng ⁷,
 L.G. Pereira ⁷³, H. Pereira Da Costa ⁷⁵, D. Peresunko ^{83,90},
 E. Perez Lezama ⁷⁰, V. Peskov ⁷⁰, Y. Pestov ⁵, V. Petráček ³⁹, V. Petrov ¹¹²,
 M. Petrovici ⁸⁷, C. Petta ²⁸, R.P. Pezzi ⁷³, S. Piano ⁵⁹, M. Pikna ³⁸,
 P. Pillot ¹¹⁴, L.O.D.L. Pimentel ⁹¹, O. Pinazza ^{53,35}, L. Pinsky ¹²⁴,
 D.B. Piyarathna ¹²⁴, M. Płoskoń ⁸², M. Planinic ⁹⁸, F. Pliquet ⁷⁰,
 J. Pluta ¹³⁸, S. Pochybova ¹⁴⁰, P.L.M. Podesta-Lerma ¹²⁰,
 M.G. Poghosyan ⁹⁵, B. Polichtchouk ¹¹², N. Poljak ⁹⁸, W. Poonsawat ¹¹⁵,
 A. Pop ⁸⁷, H. Poppenborg ⁷¹, S. Porteboeuf-Houssais ¹³¹, V. Pozdniakov ⁷⁷,
 S.K. Prasad ⁴, R. Preghenella ⁵³, F. Prino ⁵⁸, C.A. Pruneau ¹³⁹,
 I. Pshenichnov ⁶², M. Puccio ²⁶, V. Punin ¹⁰⁸, J. Putschke ¹³⁹, S. Raha ⁴,
 S. Rajput ¹⁰¹, J. Rak ¹²⁵, A. Rakotozafindrabe ⁷⁵, L. Ramello ³², F. Rami ¹³³,
 D.B. Rana ¹²⁴, R. Raniwala ¹⁰², S. Raniwala ¹⁰², S.S. Räsänen ⁴⁶,
 B.T. Rascanu ⁷⁰, D. Rathee ⁹⁹, V. Ratza ⁴⁵, I. Ravasenga ³¹, K.F. Read ^{127,95},
 K. Redlich ^{86,v}, A. Rehman ²², P. Reichelt ⁷⁰, F. Reidt ³⁵, X. Ren ⁷,
 R. Renfordt ⁷⁰, A. Reshetin ⁶², K. Reygers ¹⁰⁴, V. Riabov ⁹⁶, T. Richert ^{34,63},
 M. Richter ²¹, P. Riedler ³⁵, W. Riegler ³⁵, F. Riggi ²⁸, C. Ristea ⁶⁸,
 M. Rodríguez Cahuantzi ², K. Røed ²¹, E. Rogochaya ⁷⁷, D. Rohr ^{35,42},
 D. Röhrich ²², P.S. Rokita ¹³⁸, F. Ronchetti ⁵¹, E.D. Rosas ⁷², P. Rosnet ¹³¹,
 A. Rossi ^{29,56}, A. Rotondi ¹³⁴, F. Roukoutakis ⁸⁵, C. Roy ¹³³, P. Roy ¹⁰⁹,

- A.J. Rubio Montero ¹⁰, O.V. Rueda ⁷², R. Rui ²⁵, B. Rumyantsev ⁷⁷,
 A. Rustamov ⁸⁹, E. Ryabinkin ⁹⁰, Y. Ryabov ⁹⁶, A. Rybicki ¹¹⁸,
 S. Saarinen ⁴⁶, S. Sadhu ¹³⁷, S. Sadovsky ¹¹², K. Šafařík ³⁵, S.K. Saha ¹³⁷,
 B. Sahlmuller ⁷⁰, B. Sahoo ⁴⁸, P. Sahoo ⁴⁹, R. Sahoo ⁴⁹, S. Sahoo ⁶⁷,
 P.K. Sahu ⁶⁷, J. Saini ¹³⁷, S. Sakai ¹³⁰, M.A. Saleh ¹³⁹, J. Salzwedel ¹⁸,
 S. Sambyal ¹⁰¹, V. Samsonov ^{96,83}, A. Sandoval ⁷⁴, A. Sarkar ⁷⁶,
 D. Sarkar ¹³⁷, N. Sarkar ¹³⁷, P. Sarma ⁴⁴, M.H.P. Sas ⁶³, E. Scapparone ⁵³,
 F. Scarlassara ²⁹, B. Schaefer ⁹⁵, H.S. Scheid ⁷⁰, C. Schiaua ⁸⁷,
 R. Schicker ¹⁰⁴, C. Schmidt ¹⁰⁶, H.R. Schmidt ¹⁰³, M.O. Schmidt ¹⁰⁴,
 M. Schmidt ¹⁰³, N.V. Schmidt ^{95,70}, J. Schukraft ³⁵, Y. Schutz ^{35,133},
 K. Schwarz ¹⁰⁶, K. Schweda ¹⁰⁶, G. Scioli ²⁷, E. Scomparin ⁵⁸, M. Šefčík ⁴⁰,
 J.E. Seger ⁹⁷, Y. Sekiguchi ¹²⁹, D. Sekihata ⁴⁷, I. Selyuzhenkov ^{106,83},
 K. Senosi ⁷⁶, S. Senyukov ¹³³, E. Serradilla ^{74,10}, P. Sett ⁴⁸, A. Sevcenco ⁶⁸,
 A. Shabanov ⁶², A. Shabetai ¹¹⁴, R. Shahoyan ³⁵, W. Shaikh ¹⁰⁹,
 A. Shangaraev ¹¹², A. Sharma ⁹⁹, A. Sharma ¹⁰¹, M. Sharma ¹⁰¹,
 M. Sharma ¹⁰¹, N. Sharma ⁹⁹, A.I. Sheikh ¹³⁷, K. Shigaki ⁴⁷, S. Shirinkin ⁶⁴,
 Q. Shou ⁷, K. Shtejer ^{9,26}, Y. Sibirskiak ⁹⁰, S. Siddhanta ⁵⁴, K.M. Sielewicz ³⁵,
 T. Siemiaczuk ⁸⁶, S. Silaeva ⁹⁰, D. Silvermyr ³⁴, G. Simatovic ⁹²,
 G. Simonetti ³⁵, R. Singaraju ¹³⁷, R. Singh ⁸⁸, V. Singhal ¹³⁷, T. Sinha ¹⁰⁹,
 B. Sitar ³⁸, M. Sitta ³², T.B. Skaali ²¹, M. Slupecki ¹²⁵, N. Smirnov ¹⁴¹,
 R.J.M. Snellings ⁶³, T.W. Snellman ¹²⁵, J. Song ¹⁹, M. Song ¹⁴²,
 F. Soramel ²⁹, S. Sorensen ¹²⁷, F. Sozzi ¹⁰⁶, I. Sputowska ¹¹⁸, J. Stachel ¹⁰⁴,
 I. Stan ⁶⁸, P. Stankus ⁹⁵, E. Stenlund ³⁴, D. Stocco ¹¹⁴, M.M. Storetvedt ³⁷,
 P. Strmen ³⁸, A.A.P. Suaide ¹²¹, T. Sugitate ⁴⁷, C. Suire ⁶¹,
 M. Suleymanov ¹⁵, M. Suljic ²⁵, R. Sultanov ⁶⁴, M. Šumbera ⁹⁴,
 S. Sumowidagdo ⁵⁰, K. Suzuki ¹¹³, S. Swain ⁶⁷, A. Szabo ³⁸, I. Szarka ³⁸,
 U. Tabassam ¹⁵, J. Takahashi ¹²², G.J. Tambave ²², N. Tanaka ¹³⁰,
 M. Tarhini ⁶¹, M. Tariq ¹⁷, M.G. Tarzila ⁸⁷, A. Tauro ³⁵, G. Tejeda Muñoz ²,
 A. Telesca ³⁵, K. Terasaki ¹²⁹, C. Terrevoli ²⁹, B. Teyssier ¹³², D. Thakur ⁴⁹,
 S. Thakur ¹³⁷, D. Thomas ¹¹⁹, F. Thoresen ⁹¹, R. Tieulent ¹³²,
 A. Tikhonov ⁶², A.R. Timmins ¹²⁴, A. Toia ⁷⁰, M. Toppi ⁵¹, S.R. Torres ¹²⁰,
 S. Tripathy ⁴⁹, S. Trogolo ²⁶, G. Trombetta ³³, L. Tropp ⁴⁰, V. Trubnikov ³,
 W.H. Trzaska ¹²⁵, B.A. Trzeciak ⁶³, T. Tsuji ¹²⁹, A. Tumkin ¹⁰⁸,
 R. Turrisi ⁵⁶, T.S. Tveter ²¹, K. Ullaland ²², E.N. Umaka ¹²⁴, A. Uras ¹³²,
 G.L. Usai ²⁴, A. Utrobinicic ⁹⁸, M. Vala ^{116,65}, J. Van Der Maarel ⁶³,
 J.W. Van Hoorne ³⁵, M. van Leeuwen ⁶³, T. Vanat ⁹⁴, P. Vande Vyvre ³⁵,
 D. Varga ¹⁴⁰, A. Vargas ², M. Vargyas ¹²⁵, R. Varma ⁴⁸, M. Vasileiou ⁸⁵,

- A. Vasiliev ⁹⁰, A. Vauthier ⁸¹, O. Vázquez Doce ^{105,36}, V. Vechernin ¹³⁶,
 A.M. Veen ⁶³, A. Velure ²², E. Vercellin ²⁶, S. Vergara Limón ², R. Vernet ⁸,
 R. Vértesi ¹⁴⁰, L. Vickovic ¹¹⁷, S. Vigolo ⁶³, J. Viinikainen ¹²⁵,
 Z. Vilakazi ¹²⁸, O. Villalobos Baillie ¹¹⁰, A. Villatoro Tello ²,
 A. Vinogradov ⁹⁰, L. Vinogradov ¹³⁶, T. Virgili ³⁰, V. Vislavicius ³⁴,
 A. Vodopyanov ⁷⁷, M.A. Völkl ¹⁰³, K. Voloshin ⁶⁴, S.A. Voloshin ¹³⁹,
 G. Volpe ³³, B. von Haller ³⁵, I. Vorobyev ^{105,36}, D. Voscek ¹¹⁶,
 D. Vranic ^{35,106}, J. Vrláková ⁴⁰, B. Wagner ²², H. Wang ⁶³, M. Wang ⁷,
 D. Watanabe ¹³⁰, Y. Watanabe ^{129,130}, M. Weber ¹¹³, S.G. Weber ¹⁰⁶,
 D.F. Weiser ¹⁰⁴, S.C. Wenzel ³⁵, J.P. Wessels ⁷¹, U. Westerhoff ⁷¹,
 A.M. Whitehead ¹⁰⁰, J. Wiechula ⁷⁰, J. Wikne ²¹, G. Wilk ⁸⁶,
 J. Wilkinson ^{104,53}, G.A. Willems ^{35,71}, M.C.S. Williams ⁵³, E. Willsher ¹¹⁰,
 B. Windelband ¹⁰⁴, W.E. Witt ¹²⁷, R. Xu ⁷, S. Yalcin ⁸⁰, K. Yamakawa ⁴⁷,
 P. Yang ⁷, S. Yano ⁴⁷, Z. Yin ⁷, H. Yokoyama ^{130,81}, I.-K. Yoo ¹⁹,
 J.H. Yoon ⁶⁰, E. Yun ¹⁹, V. Yurchenko ³, V. Zaccolo ⁵⁸, A. Zaman ¹⁵,
 C. Zampolli ³⁵, H.J.C. Zanolli ¹²¹, N. Zardoshti ¹¹⁰, A. Zarochentsev ¹³⁶,
 P. Závada ⁶⁶, N. Zaviyalov ¹⁰⁸, H. Zbroszczyk ¹³⁸, M. Zhalov ⁹⁶,
 H. Zhang ^{22,7}, X. Zhang ⁷, Y. Zhang ⁷, C. Zhang ⁶³, Z. Zhang ^{7,131},
 C. Zhao ²¹, N. Zhigareva ⁶⁴, D. Zhou ⁷, Y. Zhou ⁹¹, Z. Zhou ²², H. Zhu ²²,
 J. Zhu ⁷, Y. Zhu ⁷, A. Zichichi ^{12,27}, M.B. Zimmermann ³⁵, G. Zinovjev ³,
 J. Zmeskal ¹¹³, S. Zou ⁷

¹ A.I. Alikhanyan National Science Laboratory (Yerevan Physics Institute) Foundation, Yerevan, Armenia² Benemérita Universidad Autónoma de Puebla, Puebla, Mexico³ Bogolyubov Institute for Theoretical Physics, Kiev, Ukraine⁴ Bose Institute, Department of Physics and Centre for Astroparticle Physics and Space Science (CAPSS), Kolkata, India⁵ Budker Institute for Nuclear Physics, Novosibirsk, Russia⁶ California Polytechnic State University, San Luis Obispo, CA, United States⁷ Central China Normal University, Wuhan, China⁸ Centre de Calcul de l'IN2P3, Villeurbanne, Lyon, France⁹ Centro de Aplicaciones Tecnológicas y Desarrollo Nuclear (CEADEN), Havana, Cuba¹⁰ Centro de Investigaciones Energéticas Medioambientales y Tecnológicas (CIEMAT), Madrid, Spain¹¹ Centro de Investigación y de Estudios Avanzados (CINVESTAV), Mexico City and Mérida, Mexico¹² Centro Fermi – Museo Storico della Fisica e Centro Studi e Ricerche ‘Enrico Fermi’, Rome, Italy¹³ Chicago State University, Chicago, IL, United States¹⁴ China Institute of Atomic Energy, Beijing, China¹⁵ COMSATS Institute of Information Technology (CIIT), Islamabad, Pakistan¹⁶ Departamento de Física de Partículas and IGFAE, Universidad de Santiago de Compostela, Santiago de Compostela, Spain¹⁷ Department of Physics, Aligarh Muslim University, Aligarh, India¹⁸ Department of Physics, Ohio State University, Columbus, OH, United States¹⁹ Department of Physics, Pusan National University, Pusan, Republic of Korea²⁰ Department of Physics, Sejong University, Seoul, Republic of Korea²¹ Department of Physics, University of Oslo, Oslo, Norway²² Department of Physics and Technology, University of Bergen, Bergen, Norway

- ²³ Dipartimento di Fisica dell'Università 'La Sapienza' and Sezione INFN, Rome, Italy
²⁴ Dipartimento di Fisica dell'Università and Sezione INFN, Cagliari, Italy
²⁵ Dipartimento di Fisica dell'Università and Sezione INFN, Trieste, Italy
²⁶ Dipartimento di Fisica dell'Università and Sezione INFN, Turin, Italy
²⁷ Dipartimento di Fisica e Astronomia dell'Università and Sezione INFN, Bologna, Italy
²⁸ Dipartimento di Fisica e Astronomia dell'Università and Sezione INFN, Catania, Italy
²⁹ Dipartimento di Fisica e Astronomia dell'Università and Sezione INFN, Padova, Italy
³⁰ Dipartimento di Fisica 'E.R. Caianiello' dell'Università and Gruppo Collegato INFN, Salerno, Italy
³¹ Dipartimento DISAT del Politecnico and Sezione INFN, Turin, Italy
³² Dipartimento di Scienze e Innovazione Tecnologica dell'Università del Piemonte Orientale and INFN Sezione di Torino, Alessandria, Italy
³³ Dipartimento Interateneo di Fisica 'M. Merlin' and Sezione INFN, Bari, Italy
³⁴ Division of Experimental High Energy Physics, University of Lund, Lund, Sweden
³⁵ European Organization for Nuclear Research (CERN), Geneva, Switzerland
³⁶ Excellence Cluster Universe, Technische Universität München, Munich, Germany
³⁷ Faculty of Engineering, Bergen University College, Bergen, Norway
³⁸ Faculty of Mathematics, Physics and Informatics, Comenius University, Bratislava, Slovakia
³⁹ Faculty of Nuclear Sciences and Physical Engineering, Czech Technical University in Prague, Prague, Czech Republic
⁴⁰ Faculty of Science, P.J. Šafárik University, Košice, Slovakia
⁴¹ Faculty of Technology, Buskerud and Vestfold University College, Tønsberg, Norway
⁴² Frankfurt Institute for Advanced Studies, Johann Wolfgang Goethe-Universität Frankfurt, Frankfurt, Germany
⁴³ Gangneung-Wonju National University, Gangneung, Republic of Korea
⁴⁴ Gauhati University, Department of Physics, Guwahati, India
⁴⁵ Helmholtz-Institut für Strahlen- und Kernphysik, Rheinische Friedrich-Wilhelms-Universität Bonn, Bonn, Germany
⁴⁶ Helsinki Institute of Physics (HIP), Helsinki, Finland
⁴⁷ Hiroshima University, Hiroshima, Japan
⁴⁸ Indian Institute of Technology Bombay (IIT), Mumbai, India
⁴⁹ Indian Institute of Technology Indore, Indore, India
⁵⁰ Indonesian Institute of Sciences, Jakarta, Indonesia
⁵¹ INFN, Laboratori Nazionali di Frascati, Frascati, Italy
⁵² INFN, Sezione di Bari, Bari, Italy
⁵³ INFN, Sezione di Bologna, Bologna, Italy
⁵⁴ INFN, Sezione di Cagliari, Cagliari, Italy
⁵⁵ INFN, Sezione di Catania, Catania, Italy
⁵⁶ INFN, Sezione di Padova, Padova, Italy
⁵⁷ INFN, Sezione di Roma, Rome, Italy
⁵⁸ INFN, Sezione di Torino, Turin, Italy
⁵⁹ INFN, Sezione di Trieste, Trieste, Italy
⁶⁰ Inha University, Incheon, Republic of Korea
⁶¹ Institut de Physique Nucléaire d'Orsay (IPNO), Université Paris-Sud, CNRS-IN2P3, Orsay, France
⁶² Institute for Nuclear Research, Academy of Sciences, Moscow, Russia
⁶³ Institute for Subatomic Physics of Utrecht University, Utrecht, Netherlands
⁶⁴ Institute for Theoretical and Experimental Physics, Moscow, Russia
⁶⁵ Institute of Experimental Physics, Slovak Academy of Sciences, Košice, Slovakia
⁶⁶ Institute of Physics, Academy of Sciences of the Czech Republic, Prague, Czech Republic
⁶⁷ Institute of Physics, Bhubaneswar, India
⁶⁸ Institute of Space Science (ISS), Bucharest, Romania
⁶⁹ Institut für Informatik, Johann Wolfgang Goethe-Universität Frankfurt, Frankfurt, Germany
⁷⁰ Institut für Kernphysik, Johann Wolfgang Goethe-Universität Frankfurt, Frankfurt, Germany
⁷¹ Institut für Kernphysik, Westfälische Wilhelms-Universität Münster, Münster, Germany
⁷² Instituto de Ciencias Nucleares, Universidad Nacional Autónoma de México, Mexico City, Mexico
⁷³ Instituto de Física, Universidade Federal do Rio Grande do Sul (UFRGS), Porto Alegre, Brazil
⁷⁴ Instituto de Física, Universidad Nacional Autónoma de México, Mexico City, Mexico
⁷⁵ IRFU, CEA, Université Paris-Saclay, Saclay, France
⁷⁶ iThemba LABS, National Research Foundation, Somerset West, South Africa

- ⁷⁷ Joint Institute for Nuclear Research (JINR), Dubna, Russia
⁷⁸ Konkuk University, Seoul, Republic of Korea
⁷⁹ Korea Institute of Science and Technology Information, Daejeon, Republic of Korea
⁸⁰ KTO Karatay University, Konya, Turkey
⁸¹ Laboratoire de Physique Subatomique et de Cosmologie, Université Grenoble-Alpes, CNRS-IN2P3, Grenoble, France
⁸² Lawrence Berkeley National Laboratory, Berkeley, CA, United States
⁸³ Moscow Engineering Physics Institute, Moscow, Russia
⁸⁴ Nagasaki Institute of Applied Science, Nagasaki, Japan
⁸⁵ National and Kapodistrian University of Athens, Physics Department, Athens, Greece
⁸⁶ National Centre for Nuclear Studies, Warsaw, Poland
⁸⁷ National Institute for Physics and Nuclear Engineering, Bucharest, Romania
⁸⁸ National Institute of Science Education and Research, HBNI, Jatni, India
⁸⁹ National Nuclear Research Center, Baku, Azerbaijan
⁹⁰ National Research Centre Kurchatov Institute, Moscow, Russia
⁹¹ Niels Bohr Institute, University of Copenhagen, Copenhagen, Denmark
⁹² Nikhef, Nationaal instituut voor subatomaire fysica, Amsterdam, Netherlands
⁹³ Nuclear Physics Group, STFC Daresbury Laboratory, Daresbury, United Kingdom
⁹⁴ Nuclear Physics Institute, Academy of Sciences of the Czech Republic, Řež u Prahy, Czech Republic
⁹⁵ Oak Ridge National Laboratory, Oak Ridge, TN, United States
⁹⁶ Petersburg Nuclear Physics Institute, Gatchina, Russia
⁹⁷ Physics Department, Creighton University, Omaha, NE, United States
⁹⁸ Physics Department, Faculty of Science, University of Zagreb, Zagreb, Croatia
⁹⁹ Physics Department, Panjab University, Chandigarh, India
¹⁰⁰ Physics Department, University of Cape Town, Cape Town, South Africa
¹⁰¹ Physics Department, University of Jammu, Jammu, India
¹⁰² Physics Department, University of Rajasthan, Jaipur, India
¹⁰³ Physikalisches Institut, Eberhard Karls Universität Tübingen, Tübingen, Germany
¹⁰⁴ Physikalisches Institut, Ruprecht-Karls-Universität Heidelberg, Heidelberg, Germany
¹⁰⁵ Physik Department, Technische Universität München, Munich, Germany
¹⁰⁶ Research Division and ExtreMe Matter Institute EMMI, GSI Helmholtzzentrum für Schwerionenforschung GmbH, Darmstadt, Germany
¹⁰⁷ Rudjer Bošković Institute, Zagreb, Croatia
¹⁰⁸ Russian Federal Nuclear Center (VNIIEF), Sarov, Russia
¹⁰⁹ Saha Institute of Nuclear Physics, Kolkata, India
¹¹⁰ School of Physics and Astronomy, University of Birmingham, Birmingham, United Kingdom
¹¹¹ Sección Física, Departamento de Ciencias, Pontificia Universidad Católica del Perú, Lima, Peru
¹¹² SSC IHEP of NRC Kurchatov institute, Protvino, Russia
¹¹³ Stefan Meyer Institut für Subatomare Physik (SMI), Vienna, Austria
¹¹⁴ SUBATECH, IMT Atlantique, Université de Nantes, CNRS-IN2P3, Nantes, France
¹¹⁵ Suranaree University of Technology, Nakhon Ratchasima, Thailand
¹¹⁶ Technical University of Košice, Košice, Slovakia
¹¹⁷ Technical University of Split FESB, Split, Croatia
¹¹⁸ The Henryk Niewodniczanski Institute of Nuclear Physics, Polish Academy of Sciences, Cracow, Poland
¹¹⁹ The University of Texas at Austin, Physics Department, Austin, TX, United States
¹²⁰ Universidad Autónoma de Sinaloa, Culiacán, Mexico
¹²¹ Universidade de São Paulo (USP), São Paulo, Brazil
¹²² Universidade Estadual de Campinas (UNICAMP), Campinas, Brazil
¹²³ Universidade Federal do ABC, Santo Andre, Brazil
¹²⁴ University of Houston, Houston, TX, United States
¹²⁵ University of Jyväskylä, Jyväskylä, Finland
¹²⁶ University of Liverpool, Liverpool, United Kingdom
¹²⁷ University of Tennessee, Knoxville, TN, United States
¹²⁸ University of the Witwatersrand, Johannesburg, South Africa
¹²⁹ University of Tokyo, Tokyo, Japan
¹³⁰ University of Tsukuba, Tsukuba, Japan

- ¹³¹ Université Clermont Auvergne, CNRS/IN2P3, LPC, Clermont-Ferrand, France
¹³² Université de Lyon, Université Lyon 1, CNRS/IN2P3, IPN-Lyon, Villeurbanne, Lyon, France
¹³³ Université de Strasbourg, CNRS, IPHC UMR 7178, F-67000 Strasbourg, France
¹³⁴ Università degli Studi di Pavia, Pavia, Italy
¹³⁵ Università di Brescia, Brescia, Italy
¹³⁶ V. Fock Institute for Physics, St. Petersburg State University, St. Petersburg, Russia
¹³⁷ Variable Energy Cyclotron Centre, Kolkata, India
¹³⁸ Warsaw University of Technology, Warsaw, Poland
¹³⁹ Wayne State University, Detroit, MI, United States
¹⁴⁰ Wigner Research Centre for Physics, Hungarian Academy of Sciences, Budapest, Hungary
¹⁴¹ Yale University, New Haven, CT, United States
¹⁴² Yonsei University, Seoul, Republic of Korea
¹⁴³ Zentrum für Technologietransfer und Telekommunikation (ZTT), Fachhochschule Worms, Worms, Germany

ⁱ Deceased.

ⁱⁱ Dipartimento DET del Politecnico di Torino, Turin, Italy.

ⁱⁱⁱ M.V. Lomonosov Moscow State University, D.V. Skobeltsyn Institute of Nuclear Physics, Moscow, Russia.

^{iv} Department of Applied Physics, Aligarh Muslim University, Aligarh, India.

^v Institute of Theoretical Physics, University of Wroclaw, Poland.